J Korean Med Sci. 2019 Mar 4;34(8):e66
https://doi.org/10.3346/jkms.2019.34.e66
eISSN 1598-6357·pISSN 1011-8934

JKMS

Original Article
Global Health

Check for updates

Rise of the Visible Monkey: Sectioned Images of Rhesus Monkey

Beom Sun Chung,[1] **Chang-Yeop Jeon**,[2] **Jae-Won Huh**,[2,3] **Kang-Jin Jeong**,[2] **Donghwan Har**,[4] **Kyu-Sung Kwack**,[5] **and Jin Seo Park**[6]

[1]Department of Anatomy, Ajou University School of Medicine, Suwon, Korea
[2]National Primate Research Center, Korea Research Institute of Bioscience and Biotechnology, Cheongju, Korea
[3]Department of Functional Genomics, KRIBB School of Bioscience, Korea University of Science and Technology, Daejeon, Korea
[4]College of ICT Engineering, Chung Ang University, Seoul, Korea
[5]Department of Radiology, Ajou University School of Medicine, Suwon, Korea
[6]Department of Anatomy, Dongguk University School of Medicine, Gyeongju, Korea

OPEN ACCESS

Received: Nov 13, 2018
Accepted: Jan 29, 2019

Address for Correspondence:
Jin Seo Park, PhD
Department of Anatomy, Dongguk University School of Medicine, 87 Dongdae-ro, Gyeongju 38067, Republic of Korea.
E-mail: park93@dongguk.ac.kr

ORCID iDs
Beom Sun Chung
https://orcid.org/0000-0002-3644-9120
Chang-Yeop Jeon
https://orcid.org/0000-0002-8229-7068
Jae-Won Huh
https://orcid.org/0000-0001-5845-939X
Kang-Jin Jeong
https://orcid.org/0000-0001-9824-3382
Donghwan Har
https://orcid.org/0000-0002-8676-8242
Kyu-Sung Kwack
https://orcid.org/0000-0001-6124-8948
Jin Seo Park
https://orcid.org/0000-0001-7956-4148

Funding
This research was financially supported by the Ministry of Trade, Industry and Energy

ABSTRACT

Background: Gross anatomy and sectional anatomy of a monkey should be known by students and researchers of veterinary medicine and medical research. However, materials to learn the anatomy of a monkey are scarce. Thus, the objective of this study was to produce a Visible Monkey data set containing cross sectional images, computed tomographs (CTs), and magnetic resonance images (MRIs) of a monkey whole body.
Methods: Before and after sacrifice, a female rhesus monkey was used for 3 Tesla MRI and CT scanning. The monkey was frozen and sectioned at 0.05 mm intervals for the head region and at 0.5 mm intervals for the rest of the body using a cryomacrotome. Each sectioned surface was photographed using a digital camera to obtain horizontal sectioned images. Segmentation of sectioned images was performed to elaborate three-dimensional (3D) models of the skin and brain.
Results: A total of 1,612 horizontal sectioned images of the head and 1,355 images of the remaining region were obtained. The small pixel size (0.024 mm × 0.024 mm) and real color (48 bits color) of these images enabled observations of minute structures.
Conclusion: Due to small intervals of these images, continuous structures could be traced completely. Moreover, 3D models of the skin and brain could be used for virtual dissections. Sectioned images of this study will enhance the understanding of monkey anatomy and foster further studies. These images will be provided to any requesting researcher free of charge.

Keywords: Cross Sectional Anatomy; Magnetic Resonance Imaging; Monkey; Primates; Visible Human Project

INTRODUCTION

Monkeys are used significantly in various studies of veterinary medicine and human medicine, owing to their similarities.[1-5] Therefore, veterinarians and researchers in these fields should understand the anatomy of monkeys as fundamental knowledge of the subject. However, materials for studying monkey anatomy are insufficient.[6,7] Another serious problem is that it is difficult to obtain monkeys for dissection due to required legal and ethical permissions.[8]

(MOTIE) and Korea Institute for Advancement of Technology (KIAT) through the International Cooperative R&D program (grant No. N0002249).

Disclosure

The authors have no potential conflicts of interest to disclose.

Author Contributions

Conceptualization: Park JS. Data curation: Chung BS. Investigation: Kwack KS. Resources: Jeon CY, Huh JW, Jeong KJ, Kwack KS. Software: Har D. Visualization: Har D. Writing - original draft: Chung BS.

Recently, computed tomographs (CTs) and magnetic resonance images (MRIs) of monkeys are commonly used to verify results of neuroscience studies.[9-13] To interpret CT and MRI accurately, veterinarians and researchers need to learn sectional anatomy.[14-16] Nevertheless, materials to study sectional anatomy of monkeys are insufficient. Existing sectional specimens of monkeys cannot show whole body and detailed structures together.[17] In the case of CT and MRI, it is almost impossible to produce three-dimensional (3D) models of minute structures due to low resolution and gray color.[18,19]

In the Visible Human Project, cross-sectional images of a cadaver were produced. It was a milestone, enabling observations of human body structures with high resolution and vivid colors.[20,21] Voxel-man, a 3D model made from Visible Human Project data, reached another level of realistic display of the human body.[22] After the Visible Human Project, succeeding projects to obtain improved sectioned images of cadavers were launched in Korea and China.[23-25] Using these data, numerous two-dimensional (2D) applications and 3D models of humans were developed to aid education and research of anatomy and radiology.[26-32] Once cross-sectional images in real color and 3D models of a monkey can be produced like those of humans, difficulties of real monkey dissection and shortage of materials for monkey sectional anatomy will be overcome.

To enhance the understanding of monkey anatomy, the objective of this study was to provide a Visible Monkey data set containing high quality and real color sectioned images of a rhesus monkey with corresponding CT and MRI. To achieve this purpose, the whole body of a rhesus monkey was serially ground and photographed to make sectioned images.

METHODS

A female rhesus monkey (head-to-feet length, 758 mm; weight, 4.3 kg; age at sacrifice, 93 months) was donated from the National Primate Research Center of Korea. In the state of living, the head of the monkey was 3 Tesla (3T) MR scanned using both T1 and T2 methods (repetition time, shortest; echo time, shortest). The monkey was sacrificed by an intramuscular injection of ketamine (10 mg/kg) followed by an intravenous injection of potassium chloride (100 mg/kg). Neither formalin nor dye was injected.

The sacrificed monkey was fixed on a wooden plate. Its palms were fixed to face forward to yield the anatomical position of a human. Its soles were fixed to make the ankle joint to be at a 90-degree angle. The whole body of the sacrificed monkey was scanned with CT (voltage, 140 kVp; electric current time, 240 mAs) and 3T MRI (repetition time, 675 ms; echo time, 10.944 ms).

After CT and MR scanning of the whole body, the sacrificed monkey was frozen at –70 °C for one week. After placing the monkey in gelatin solution (water 1,000 mL, gelatin 30 g, methylene blue 0.5 g) in an embedding box, the box was frozen in a freezer for one week (**Fig. 1**).[33]

The frozen monkey was serially ground with a cryomacrotome at displacement accuracy of 0.001 mm.[25]. Serial sectioning was performed at 0.05 mm intervals for the head region and at 0.5 mm intervals for the remainder of the body. After grinding, frost was wiped away using 99% ethyl alcohol. Any protruding connective tissue on the sectioned surface was removed with a scalpel (**Fig. 1**).

https://doi.org/10.3346/jkms.2019.34.e66

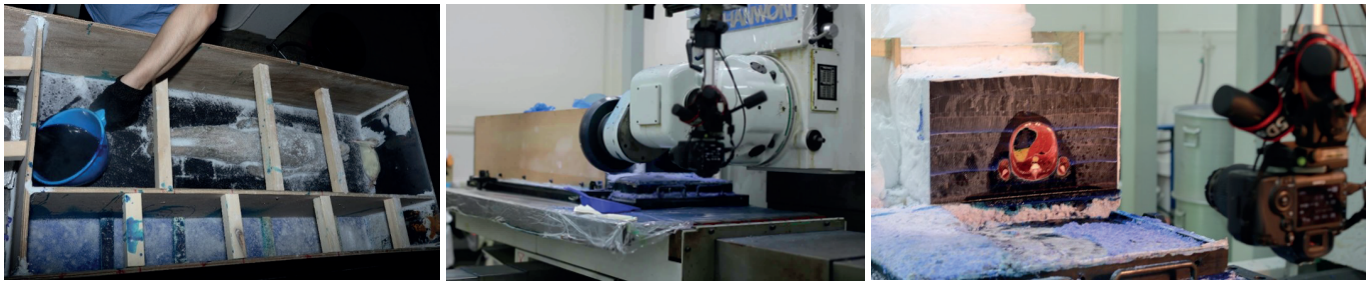

Fig. 1. Sacrificed and frozen rhesus monkey being embedded (left), serially sectioned (middle), and photographed (right).

A Canon™ EOS 5Ds R digital single-lens reflex (DSLR) camera (resolution, 8,688 × 5,792; color depth, 48 bit color) equipped with a Canon™ EF 100mm f/2.8L macro IS USM lens (Canon, Tokyo, Japan) was used. The distance from the digital camera to the sectioned surface was adjusted to provide a photograph area of 205 mm in horizontal length and 137 mm in vertical length on the sectioned surface, corresponding to a pixel size of 0.024 mm × 0.024 mm. Two strobes (Elinchrom™ digital S, Renens, Switzerland) with power pack (Elinchrom™ digital 2, Renens, Switzerland) were used to maintain constant brightness of the sectioned surface. A color control patch (Tiffen™, Hauppauge, New York, NY, USA) was placed on the sectioned surface and photographed every day for post processing of these images. The sectioned surface was photographed using a digital camera (ISO 100, shutter speed 1/250, aperture F/8, manual focus). The photograph was checked by anatomists on a computer monitor and saved in tagged image file format in Adobe Photoshop CS6 (Adobe Systems, Inc., San Jose, CA, USA). The procedure was repeated from the head to the feet (**Fig. 1**).

By post processing of these photographs,[34,35] sectioned images with consistent alignment, color, and brightness were produced. Using an in-house developed software,[36] original horizontal sectioned images were stacked and re-sectioned on a personal computer to produce coronal and sagittal images.

Ethics statement

The study protocol was reviewed and approved by the Institutional Review Board (IRB) of National Primate Research Center of Korea Research Institute of Bioscience and Biotechnology (IRB No. KRIBB-AEC-18087). Written informed consent was not required for this study.

RESULTS

After obtaining horizontal 3T MRI of the head of the living monkey, 3T MRI and CT of the whole body of the sacrificed monkey were then produced. A total of 2,967 sectioned images of the horizontal plane were manufactured without missing cuts (resolution, 8,688 × 5,792; single file size, 288 mbyte; total file size, 834 gbyte). These sectioned images were produced at 0.05 mm intervals for the head region and at 0.5 mm intervals for other regions. The pixel size was 0.024 mm × 0.024 mm and the color depth was 48-bit color (**Fig. 2** and **Table 1**). Reconstructed coronal and sagittal planes of these sectioned images revealed the whole extent of monkey anatomy (**Fig. 3**).

Extracranial and intracranial structures were clearly visible in sectioned images of the head. Eye structures including extraocular muscles and nerves were clearly visible on these images

https://doi.org/10.3346/jkms.2019.34.e66

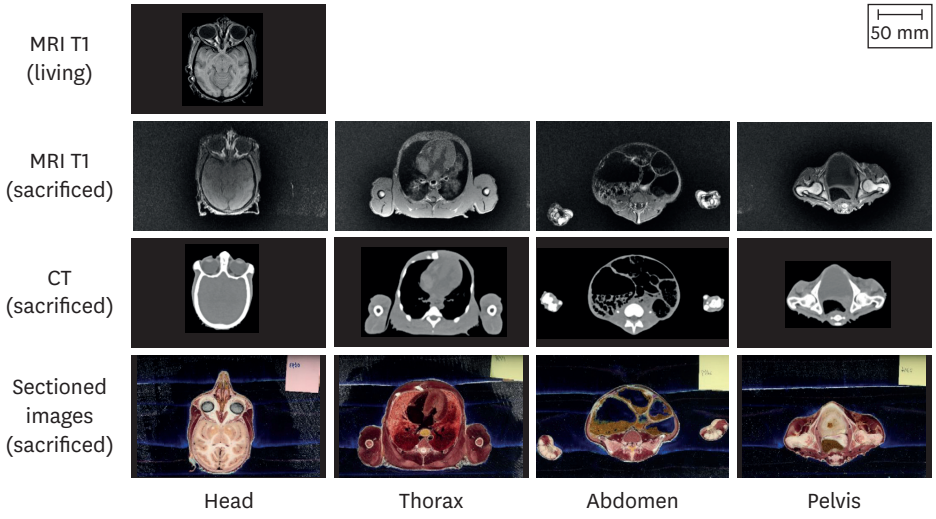

Fig. 2. MRI, CT, and sectioned images of the rhesus monkey's whole body.
MRI = magnetic resonance image, CT = computed tomography.

(**Fig. 4A**). Connection from the retina to the lateral geniculate nucleus was found (**Fig. 4A-C**). Even the reticular nucleus and external medullary lamina of the thalamus were observed on these images. The stria medullaris of the thalamus and fornix were very close to each other without touching. Eventually, the stria medullaris went to the habenula, while the fornix went to the hippocampus (**Fig. 4B-D**). Moreover, minute blood vessels were observed on these images. The nerve to the caudal rectus muscle from the oculomotor nerve was visible (**Fig. 4C and D**). The paramedian pontine perforating artery was also observed on the image (**Fig. 4E**).

In sectioned images of the thorax, the dorsal vagal trunk was found around the esophagus (**Fig. 5A**). The four chambers of the heart were identified in the middle mediastinum. In the heart, small structures such as the tendinous cord and septomarginal trabecula were visible. At the lateral side of the heart, the phrenic nerve passed the diaphragm and the coronal vessels could be observed. Moreover, the airway from the lobar bronchus to the bronchiole was visible (**Fig. 5B**). The thoracic sympathetic ganglion was thicker than the sympathetic trunk. The gray and white rami communicantes could be distinguished (**Fig. 5C**). From the left side to the right side, thoracic aorta, thoracic duct, and azygos vein were located (**Fig. 5D**). Through whole levels of the spinal cord, gray matter, white matter, spinal ganglion, ventral spinal artery, dorsal spinal artery, and even the radicular artery were all clearly identified (**Fig. 5E**).

Table 1. Features of horizontal CT, MRI, and sectioned images of the rhesus monkey

Image	Region	Number	Resolution	Intervals, mm	Pixel size, mm	Bit depth	One file size, mbyte	Total file size, mbyte
3T MRI (T1)[a]	Head	216	640 × 640	0.5	0.5	8 bits grey	0.8	173
3T MRI (T2)[a]	Head	216	640 × 640	0.5	0.5	8 bits grey	0.6	130
3T MRI (T1)[b]	Whole body	412	1,024 × 1,024	0.5	0.5	8 bits grey	4.0	1,648
3T MRI (T2)[b]	Whole body	409	1,024 × 1,024	0.5	0.5	8 bits grey	4.0	1,636
CT[b]	Whole body	792	512 × 512	1.0	1.0	8 bits grey	1.0	792
Sectioned images[b]	Head	1,612	8,688 × 5,792	0.05	0.024	48 bits color	288.0	464,256
	Body expect head	1,355	8,688 × 5,792	0.5	0.024	48 bits color	288.0	390,240

3T = 3 Tesla, CT = computed tomography, MRI = magnetic resonance image.
[a]Monkey before death; [b]Monkey after death.

https://doi.org/10.3346/jkms.2019.34.e66

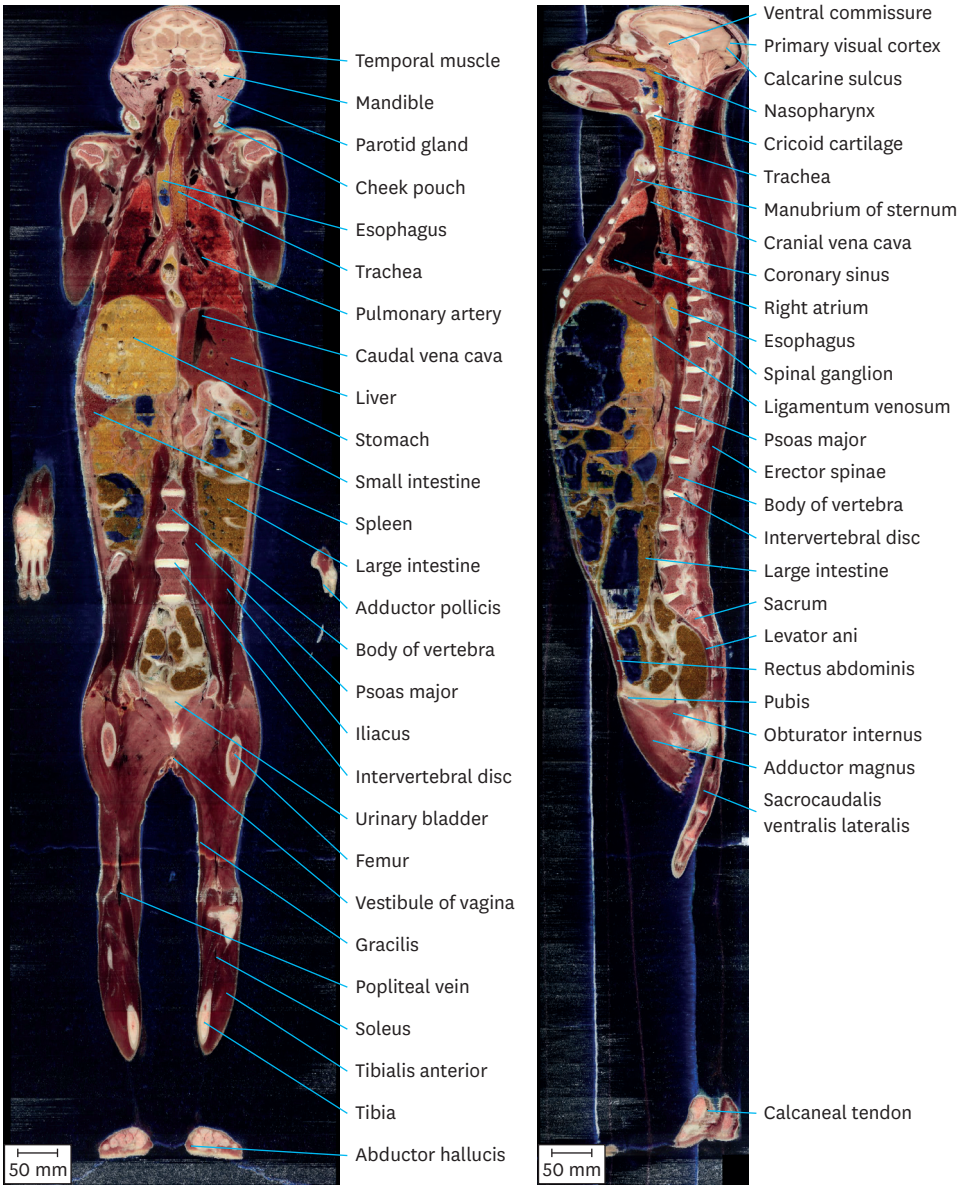

Fig. 3. Reconstructed coronal sectioned image viewed from anterior side (left) and sagittal sectioned image viewed from right side (right) of the monkey's whole body. These reconstructed images were resized proportionally regarding pixel size of the horizontal images (0.024 mm × 0.024 mm) and sectioning intervals (0.05 mm for head region and 0.5 mm for the rest).

https://doi.org/10.3346/jkms.2019.34.e66

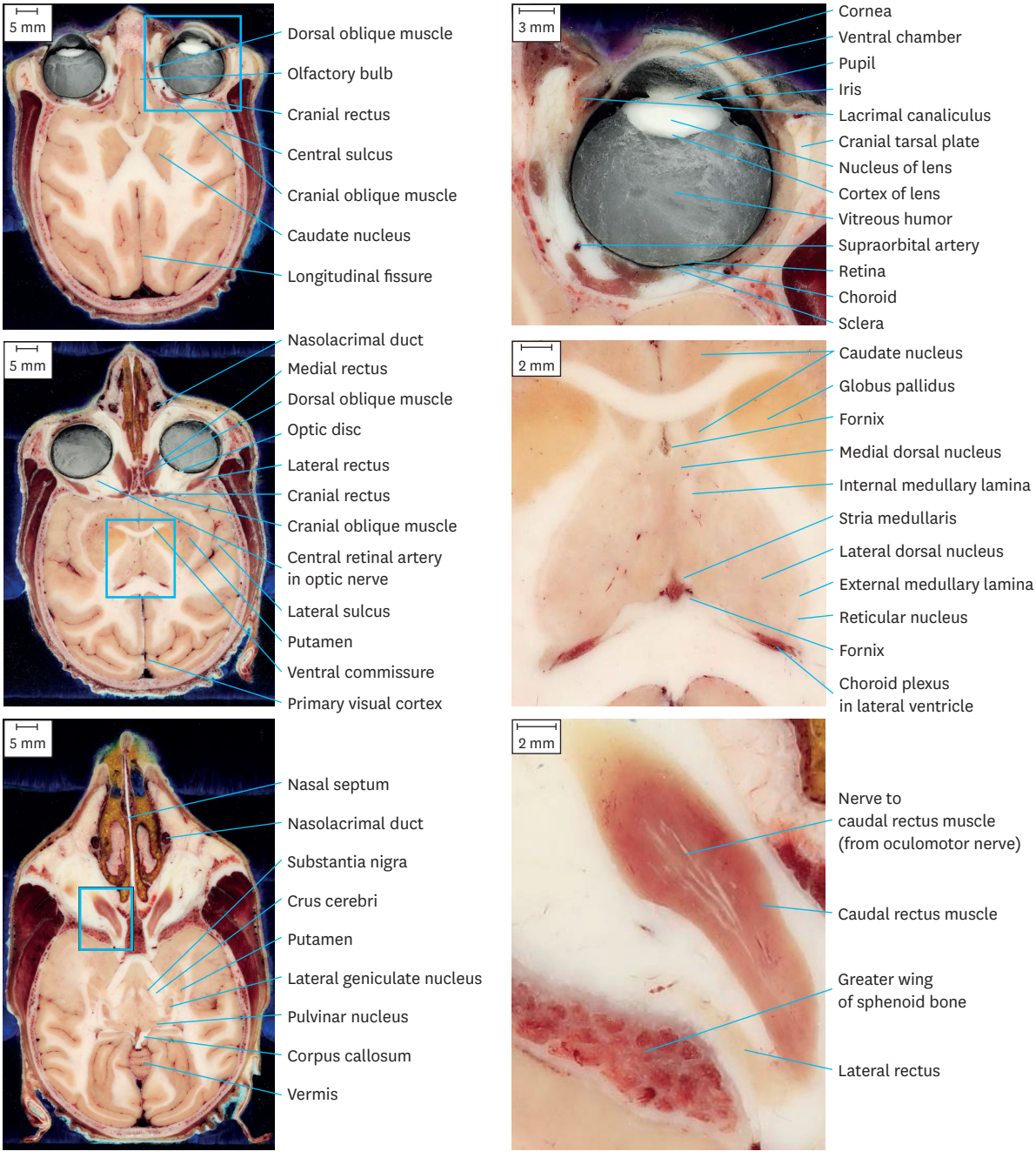

Fig. 4. Sectioned images of the head of a rhesus monkey. Images of full extent (left column) were cropped and magnified to show minute structures (right column). Levels of these images include lens (**A**), thalamus (**B**), caudal rectus muscle (**C**), midbrain (**D**), and pons (**E**). (continued to the next page)

https://doi.org/10.3346/jkms.2019.34.e66

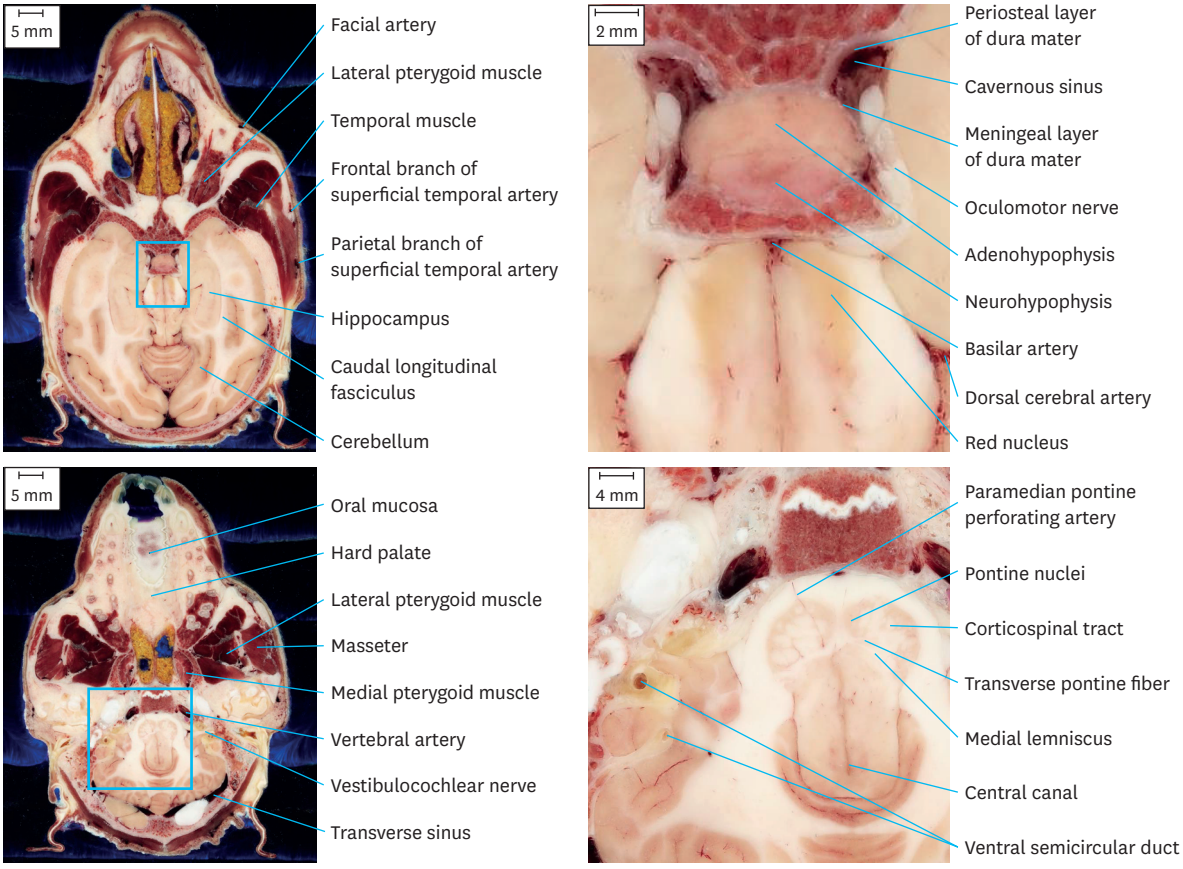

Fig. 4. (Continued) Sectioned images of the head of a rhesus monkey. Images of full extent (left column) were cropped and magnified to show minute structures (right column). Levels of these images include lens (**A**), thalamus (**B**), caudal rectus muscle (**C**), midbrain (**D**), and pons (**E**).

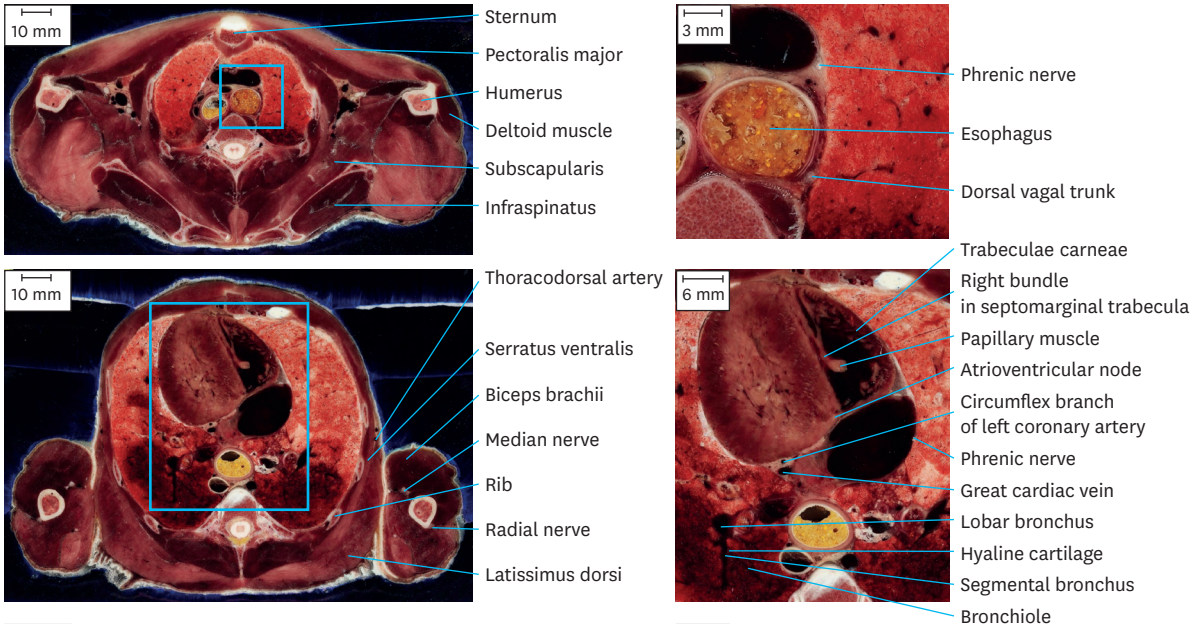

Fig. 5. Sectioned images of the thorax of a rhesus monkey. These images of full extent (left column) were cropped and magnified to show minute structures (right column). Levels of these images include the apex of the lung (**A**), upper heart (**B**), lower heart (**C**), base of the lung (**D**), and crus of the diaphragm (**E**).

(continued to the next page)

https://doi.org/10.3346/jkms.2019.34.e66

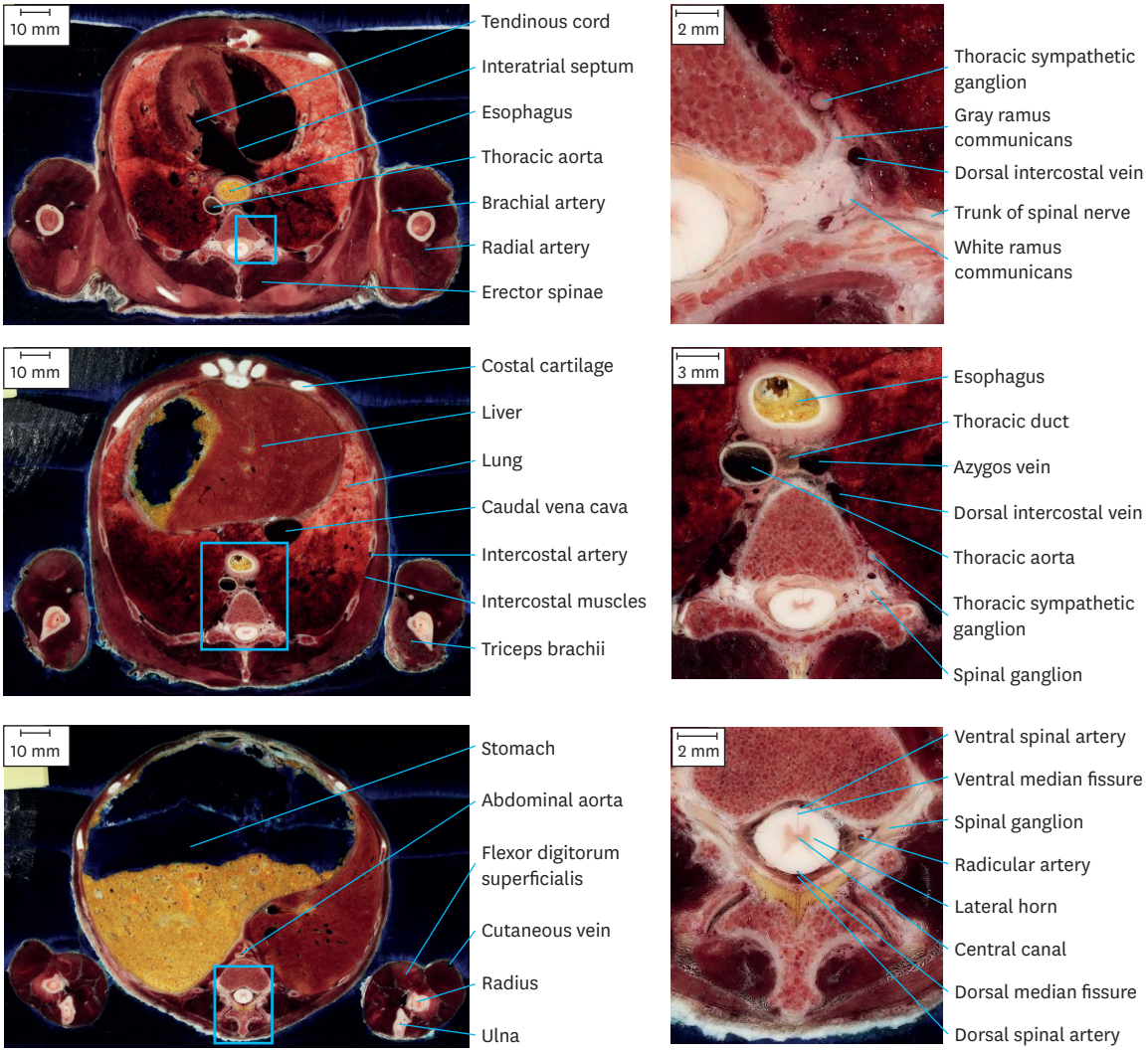

Fig. 5. (Continued) Sectioned images of the thorax of a rhesus monkey. These images of full extent (left column) were cropped and magnified to show minute structures (right column). Levels of these images include the apex of the lung (**A**), upper heart (**B**), lower heart (**C**), base of the lung (**D**), and crus of the diaphragm (**E**).

In sectioned images of the abdomen, the pancreatic duct, common bile duct, and minor duodenal papilla were identified around the duodenum. Even the gastroduodenal artery from the celiac trunk was found (**Fig. 6A**). In the kidney, minute structures including the cortical radiate vessel and minor calyx were observed (**Fig. 6B**). The central canal in the medullary cone and artery in the ventral ramus of the 5th lumbar nerve were also visible in the spinal canal (**Fig. 6C**). Regarding the pelvic structures, ovarian follicles at multiple stages were observed, owing to the specimen's young age at sacrifice (7 years old) (**Fig. 6D**). The pudendal nerve and artery were found in the pudendal canal. Cavernous structures inside the clitoris were also observed on these images (**Fig. 6F**).

Owing to the high resolution and narrow intervals of these sectioned images, whole courses of gracile structures could be traced. For example, the whole course of the sympathetic nerve (**Fig. 5C**), spinal cord with spinal nerves (**Figs. 3**, **5**, and **6**), and pancreatic ducts (**Fig. 6A**) were traced. Moreover, the right recurrent laryngeal nerve coming off from the right vagus nerve (**Fig. 7**) and the facial nerve from the stylomastoid foramen through the parotid gland

https://doi.org/10.3346/jkms.2019.34.e66

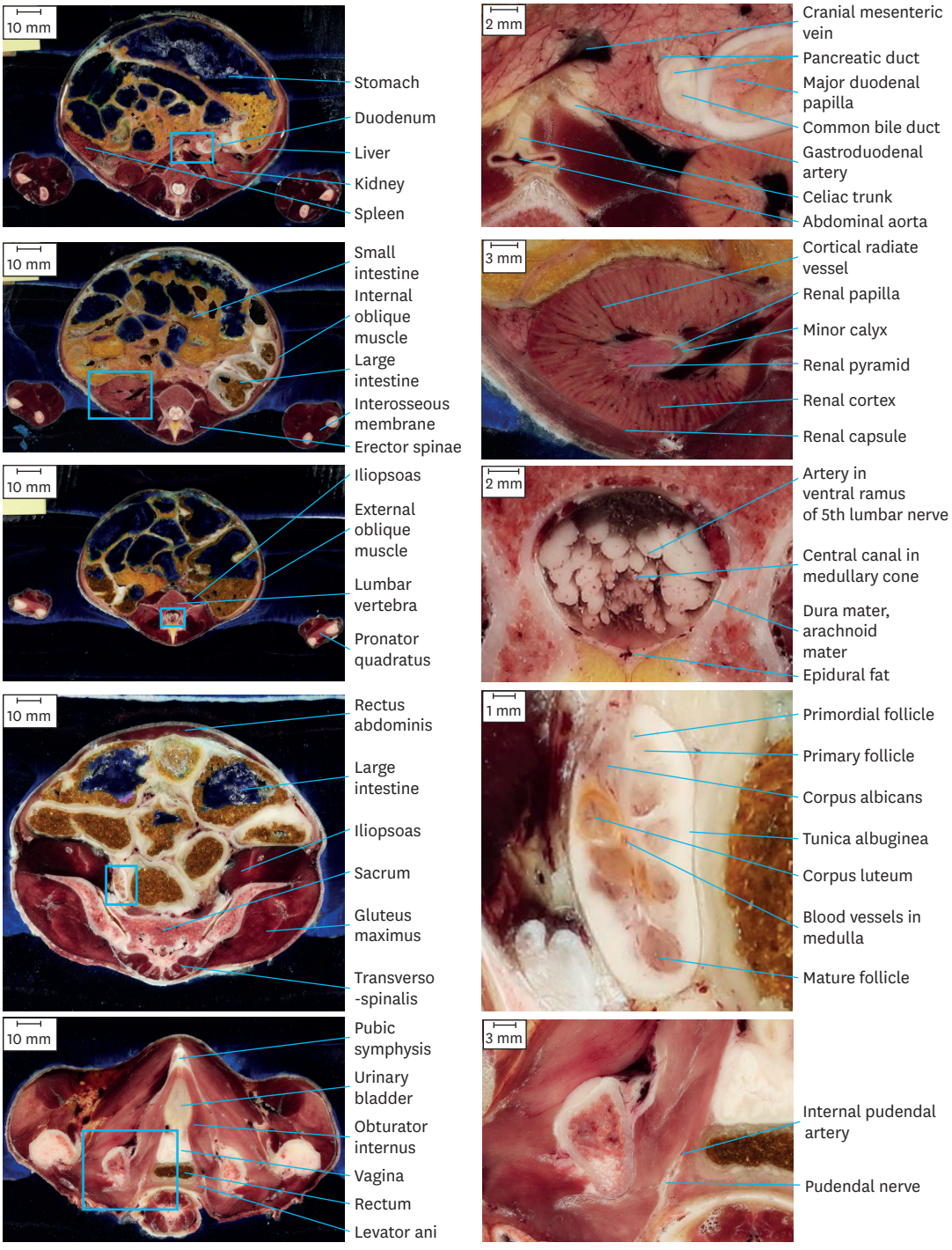

Fig. 6. Sectioned images of the abdomen and pelvis of a rhesus monkey. These images of full extent (left column) were cropped and magnified to show minute structures (right column). Levels of these images include the celiac trunk (**A**), kidney (**B**), medullary cone (**C**), ovary (**D**), pudendal canal (**E**), and clitoris (**F**).

(continued to the next page)

https://doi.org/10.3346/jkms.2019.34.e66

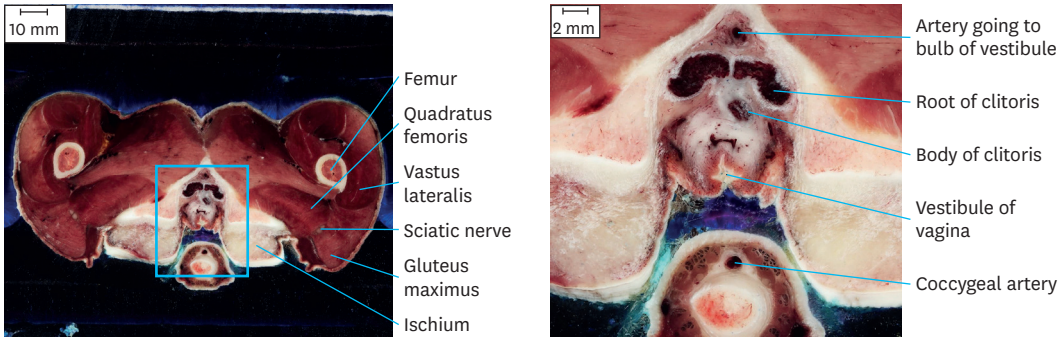

Fig. 6. (Continued) Sectioned images of the abdomen and pelvis of a rhesus monkey. These images of full extent (left column) were cropped and magnified to show minute structures (right column). Levels of these images include the celiac trunk (**A**), kidney (**B**), medullary cone (**C**), ovary (**D**), pudendal canal (**E**), and clitoris (**F**).

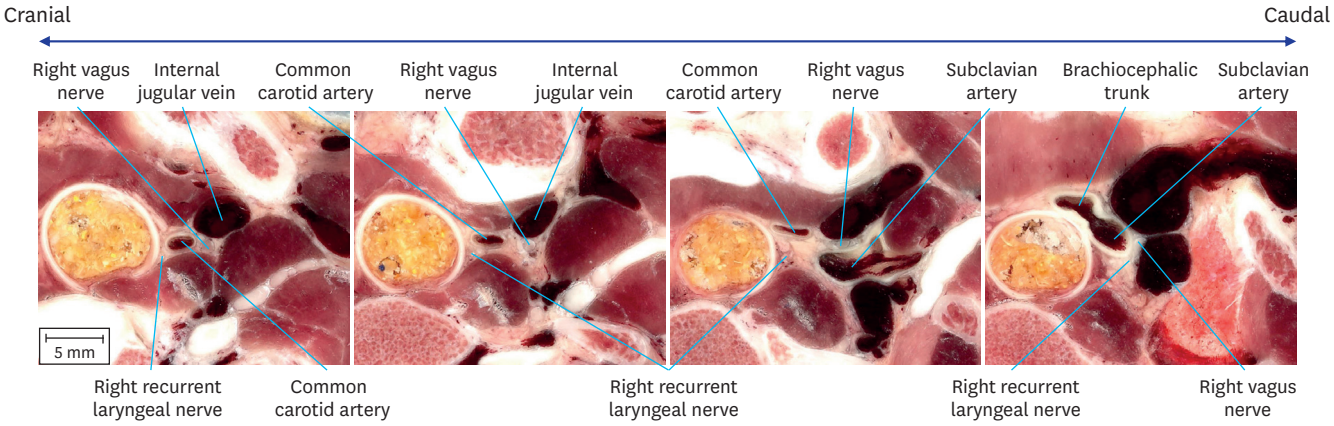

Fig. 7. Tracing the right vagus nerve branching off the right recurrent laryngeal nerve.

to the facial muscles were traced (**Fig. 8**). Similarly, any continuous structure could be traced on these serially sectioned images.

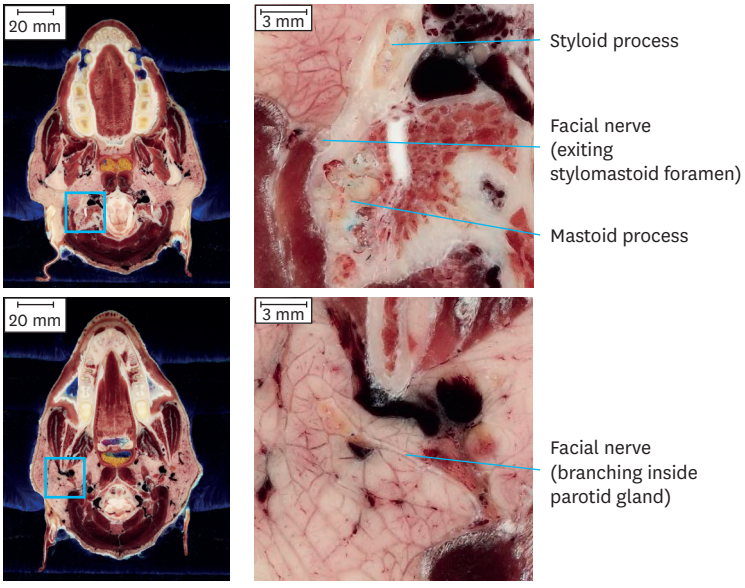

Fig. 8. Tracing the whole course of the facial nerve. These images of full extent (left column) were cropped and magnified to show minute structures (right column).

(continued to the next page)

https://doi.org/10.3346/jkms.2019.34.e66

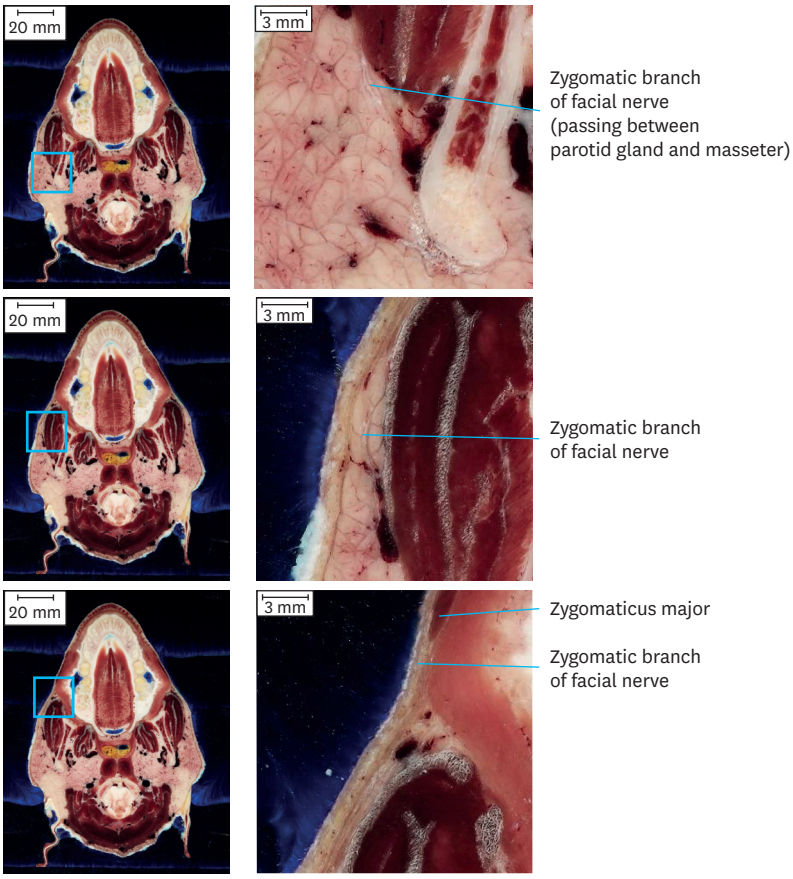

Fig. 8. (Continued) Tracing the whole course of the facial nerve. These images of full extent (left column) were cropped and magnified to show minute structures (right column).

DISCUSSION

The Visible Monkey data set of this study is the first trial to obtain high-quality and real-color sectioned images of a whole monkey body (intervals, 0.05 mm or 0.5 mm; pixel size, 0.024 mm × 0.024 mm; color depth, 48 bits color). The superb image quality enabled observations of detailed anatomical structures of a rhesus monkey (**Figs. 3-8**).

Through experience since the year 2000 in making sectioned images of humans[14,23,33,37] and animals,[38,39] the authors have accumulated several skills to yield high quality sectioned images, as follows. The first is cadaver processing skill. When receiving a donation, an appropriate specimen without lesions or prosthetics is chosen. To preserve the normal anatomy as much as possible, neither formaldehyde fixative nor dye is injected. An ideal freezing environment is formed with a deep freezer. The second is photography skills. The digital camera and lighting device are set properly according to the environment. Every sectioned surface is amended delicately. Even small flaws invisible to the naked eye are removed by observing the high-resolution photograph. The third is the post processing skill. Consistent alignment, color, and brightness of images could be achieved through post processing of these images by skilled technicians (**Fig. 3**).[34,35]

https://doi.org/10.3346/jkms.2019.34.e66

In addition to these skills, novel equipment of this study enabled high quality images. First, the cryomacrotome used in this study has high precision reliability.[23] The machine installed for previous research is still being used in the current research since 2002. Second, a high performance DSLR camera has been continuously developed by engineers.[40,41] We always utilize the newest DSLR camera. In this study, the pixel size of sectioned images was 0.024 mm by using Canon EOS 5Ds R DSLR camera, while that of previous research was 0.2 mm with Kodak DSC 560[23] and 0.1 mm with Canon EOS 5D[14] and Canon EOS-1Ds mark III.[33,38] The improvement of resolution can be verified by comparing images of this study with those of the authors' previous study.[14]

Comparative anatomy of a human and rhesus monkey is a highly interesting topic because these two species are derived from a common ancestor, catarrhini species. These sectioned images of this study will be a good source for comparative biology research.[42]

The Visible Monkey data set of this study will be upgraded continuously with segmentation and 3D reconstruction, just like the Visible Korean data set of a human.[43-45] As an initial step, the skin of the head and brain have been segmented and made into 3D models. These 3D models made from sectioned images are superior in accuracy to those made by CT or MRI. By observing these 3D models and corresponding sectioned images together, the sectional anatomy of a monkey can be elucidated in a concrete way (**Fig. 9**).

As for future steps, Visible Monkey can be used for educational purposes. By identifying numerous anatomical structures on these sectioned images, an atlas of the monkey anatomy and 3D models for a virtual dissection can be made.[16,32,33] These data sets can be also used for neuroscience research, including virtual experiment to determine effects of electromagnetic wave and radiation on an organism. The validity of the virtual experiment can be confirmed by determining if the result of the virtual experiment on a monkey corresponds to the result of an actual experiment on a monkey.[46-51]

The Visible Monkey will function as a reference for monkey anatomy. It can be used as a mutual supplementation with existing MRI and CT (**Fig. 2**). Once researchers understand monkey anatomy by using images of Visible Monkey, they can conduct studies on monkey more accurately. These data sets are expected to enhance understanding of primate studies. These images can be shared with any researcher free of charge. Researchers may send an email to the corresponding author to obtain these images.

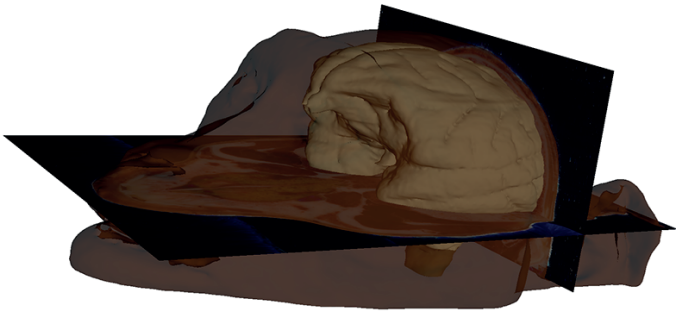

Fig. 9. Surface models of the monkey's skin and brain with embedded horizontal sectioned image and coronal sectioned image.

https://doi.org/10.3346/jkms.2019.34.e66

REFERENCES

1. Yeni-Komshian GH, Benson DA. Anatomical study of cerebral asymmetry in the temporal lobe of humans, chimpanzees, and rhesus monkeys. *Science* 1976;192(4237):387-9.
PUBMED | CROSSREF
2. Vincent JL, Patel GH, Fox MD, Snyder AZ, Baker JT, Van Essen DC, et al. Intrinsic functional architecture in the anaesthetized monkey brain. *Nature* 2007;447(7140):83-6.
PUBMED | CROSSREF
3. Jing W, Wenchao W, Lin L, Li L, Guimei W, Heng T, et al. A new MRI approach for accurately implanting microelectrodes into deep brain structures of the rhesus monkey (Macaca mulatta). *J Neurosci Methods* 2010;193(2):203-9.
PUBMED | CROSSREF
4. McBride JL, Pitzer MR, Boudreau RL, Dufour B, Hobbs T, Ojeda SR, et al. Preclinical safety of RNAi-mediated HTT suppression in the rhesus macaque as a potential therapy for Huntington's disease. *Mol Ther* 2011;19(12):2152-62.
PUBMED | CROSSREF
5. McDannold N, Arvanitis CD, Vykhodtseva N, Livingstone MS. Temporary disruption of the blood-brain barrier by use of ultrasound and microbubbles: safety and efficacy evaluation in rhesus macaques. *Cancer Res* 2012;72(14):3652-63.
PUBMED | CROSSREF
6. Hartman CG, Strauss WL, Bast TH. *The Anatomy of the Rhesus Monkey (Macaca mulatta)*. Baltimore, MD: Williams & Wilkins; 1933.
7. Berringer OM, Browning FM, Schroeder CR. *An Atlas and Dissection Manual of Rhesus Monkey Anatomy*. Tallahassee, Fl: Anatomy Laboratory Aids; 1968.
8. Kilkenny C, Browne W, Cuthill IC, Emerson M, Altman DG; NC3Rs Reporting Guidelines Working Group. Animal research: reporting in vivo experiments: the ARRIVE guidelines. *Br J Pharmacol* 2010;160(7):1577-9.
PUBMED | CROSSREF
9. Croxson PL, Johansen-Berg H, Behrens TE, Robson MD, Pinsk MA, Gross CG, et al. Quantitative investigation of connections of the prefrontal cortex in the human and macaque using probabilistic diffusion tractography. *J Neurosci* 2005;25(39):8854-66.
PUBMED | CROSSREF
10. Wisco JJ, Killiany RJ, Guttmann CR, Warfield SK, Moss MB, Rosene DL. An MRI study of age-related white and gray matter volume changes in the rhesus monkey. *Neurobiol Aging* 2008;29(10):1563-75.
PUBMED | CROSSREF
11. Mars RB, Jbabdi S, Sallet J, O'Reilly JX, Croxson PL, Olivier E, et al. Diffusion-weighted imaging tractography-based parcellation of the human parietal cortex and comparison with human and macaque resting-state functional connectivity. *J Neurosci* 2011;31(11):4087-100.
PUBMED | CROSSREF
12. Frey S, Pandya DN, Chakravarty MM, Bailey L, Petrides M, Collins DL. An MRI based average macaque monkey stereotaxic atlas and space (MNI monkey space). *Neuroimage* 2011;55(4):1435-42.
PUBMED | CROSSREF
13. Miller RE, Fowler ME. *Fowler's Zoo and Wild Animal Medicine, Volume 8*. St Louis, MO: Saunders Elsevier; 2014.
14. Park JS, Chung MS, Shin DS, Har DH, Cho ZH, Kim YB, et al. Sectioned images of the cadaver head including the brain and correspondences with ultrahigh field 7.0 T MRIs. *Proc IEEE* 2009;97(12):1988-96.
CROSSREF
15. Cho ZH. *7.0 Tesla MRI Brain Atlas: In Vivo Atlas with Cryomacrotome Correlation*. 2nd ed. New York, NY: Springer-Verlag New York; 2010.
16. Park JS. *Cross-Sectional Atlas of the Human Head: with 0.1-mm Pixel Size Color Images*. Singapore, Singapore: Springer Singapore; 2018.
17. Dauguet J. Three-dimensional histological imaging of primate brain and correlation with in vivo medical device images. *Rev Primatol* 2010;2:e4.
18. Paxinos G, Huang XF, Toga AW. *The Rhesus Monkey Brain in Stereotaxic Coordinates*. San Diego, CA: Academic Press; 2000.
19. McLaren DG, Kosmatka KJ, Oakes TR, Kroenke CD, Kohama SG, Matochik JA, et al. A population-average MRI-based atlas collection of the rhesus macaque. *Neuroimage* 2009;45(1):52-9.
PUBMED | CROSSREF

20. Spitzer V, Ackerman MJ, Scherzinger AL, Whitlock D. The visible human male: a technical report. *J Am Med Inform Assoc* 1996;3(2):118-30.
PUBMED | CROSSREF
21. Ackerman MJ. The Visible Human Project. *Proc IEEE* 1998;86(3):504-11.
22. Schiemann T, Freudenberg J, Pflesser B, Pommert A, Priesmeyer K, Riemer M, et al. Exploring the Visible Human using the VOXEL-MAN framework. *Comput Med Imaging Graph* 2000;24(3):127-32.
PUBMED | CROSSREF
23. Park JS, Chung MS, Hwang SB, Lee YS, Har DH, Park HS. Visible Korean human: improved serially sectioned images of the entire body. *IEEE Trans Med Imaging* 2005;24(3):352-60.
PUBMED | CROSSREF
24. Zhang SX, Heng PA, Liu ZJ. Chinese visible human project. *Clin Anat* 2006;19(3):204-15.
PUBMED | CROSSREF
25. Dai JX, Chung MS, Qu RM, Yuan L, Liu SW, Shin DS. The Visible Human Projects in Korea and China with improved images and diverse applications. *Surg Radiol Anat* 2012;34(6):527-34.
PUBMED | CROSSREF
26. Waldby C. *The Visible Human Project: Informatic Bodies and Posthuman Medicine*. New York, NY: Routledge; 2000.
27. Teran J, Sifakis E, Blemker SS, Ng-Thow-Hing V, Lau C, Fedkiw R. Creating and simulating skeletal muscle from the visible human data set. *IEEE Trans Vis Comput Graph* 2005;11(3):317-28.
PUBMED | CROSSREF
28. Zhang G, Luo Q, Zeng S, Liu Q. The development and application of the visible Chinese human model for Monte Carlo dose calculations. *Health Phys* 2008;94(2):118-25.
PUBMED | CROSSREF
29. Li T, Gong H, Luo Q. Visualization of light propagation in visible Chinese human head for functional near-infrared spectroscopy. *J Biomed Opt* 2011;16(4):045001.
PUBMED | CROSSREF
30. Shin DS, Chung MS, Park HS, Park JS, Hwang SB. Browsing software of the Visible Korean data used for teaching sectional anatomy. *Anat Sci Educ* 2011;4(6):327-32.
PUBMED | CROSSREF
31. Shin DS, Chung MS, Park JS, Park HS, Lee S, Moon YL, et al. Portable document format file showing the surface models of cadaver whole body. *J Korean Med Sci* 2012;27(8):849-56.
PUBMED | CROSSREF
32. Chung BS, Shin DS, Brown P, Choi J, Chung MS. Virtual dissection table including the visible Korean images, complemented by free software of the same data. *Int J Morphol* 2015;33(2):440-5.
CROSSREF
33. Park HS, Choi DH, Park JS. Improved sectioned images and surface models of the whole female body. *Int J Morphol* 2015;33(4):1323-32.
CROSSREF
34. Kim JY, Chung MS, Park JS, An CS, Har DH, Park HS. Manufacture of the serially sectioned images of the whole body (second report: photographing and processing of the anatomical images). *Korean J Anat* 2002;35(4):305-14.
35. Gonzalez RC, Woods RE, Eddins SL. *Digital Image Processing Using MATLAB*. Upper Saddle River, NJ: Pearson-Prentice-Hall; 2004.
36. Park JS, Chung MS, Park HS, Shin DS, Har DH, Cho ZH, et al. A proposal of new reference system for the standard axial, sagittal, coronal planes of brain based on the serially-sectioned images. *J Korean Med Sci* 2010;25(1):135-41.
PUBMED | CROSSREF
37. Shin DS, Jang HG, Hwang SB, Har DH, Moon YL, Chung MS. Two-dimensional sectioned images and three-dimensional surface models for learning the anatomy of the female pelvis. *Anat Sci Educ* 2013;6(5):316-23.
PUBMED | CROSSREF
38. Park HS, Shin DS, Cho DH, Jung YW, Park JS. Improved sectioned images and surface models of the whole dog body. *Ann Anat* 2014;196(5):352-9.
PUBMED | CROSSREF
39. Chung BS, Chung MS, Lee SB, Youn C, Park JS. Sectioned images of a cat head to contribute to learning of its sectional anatomy. *Int J Morphol* 2018;36(2):537-43.
CROSSREF
40. Stuurman N, Vale RD. Impact of new camera technologies on discoveries in cell biology. *Biol Bull* 2016;231(1):5-13.
PUBMED | CROSSREF

41. Cramer M, Przybilla HJ, Zurhorst A. UAV cameras: overview and geometric calibration benchmark. *ISPRS J Photogramm Remote Sens* 2017;XLII-2/W6:85-92.
CROSSREF

42. Wang Y, Cai W, Wang L, Xia R, Chen W, Zheng J, et al. Evaluation of the differences of myocardial fibers between acute and chronic myocardial infarction: application of diffusion tensor magnetic resonance imaging in a rhesus monkey model. *Korean J Radiol* 2016;17(5):725-33.
PUBMED | CROSSREF

43. Park HS, Chung MS, Shin DS, Jung YW, Park JS. Whole courses of the oculomotor, trochlear, and abducens nerves, identified in sectioned images and surface models. *Anat Rec (Hoboken)* 2015;298(2):436-43.
PUBMED | CROSSREF

44. Chung BS, Chung MS, Park JS. Six walls of the cavernous sinus identified by sectioned images and three-dimensional models: anatomic report. *World Neurosurg* 2015;84(2):337-44.
PUBMED | CROSSREF

45. Chung BS, Ahn YH, Park JS. Ten triangles around cavernous sinus for surgical approach, described by schematic diagram and three dimensional models with the sectioned images. *J Korean Med Sci* 2016;31(9):1455-63.
PUBMED | CROSSREF

46. Stewart FA, Akleyev AV, Hauer-Jensen M, Hendry JH, Kleiman NJ, Macvittie TJ, et al. ICRP publication 118: ICRP statement on tissue reactions and early and late effects of radiation in normal tissues and organs--threshold doses for tissue reactions in a radiation protection context. *Ann ICRP* 2012;41(1-2):1-322.
PUBMED | CROSSREF

47. Yeom YS, Jeong JH, Kim CH, Han MC, Ham BK, Cho KW, et al. HDRK-woman: whole-body voxel model based on high-resolution color slice images of Korean adult female cadaver. *Phys Med Biol* 2014;59(14):3969-84.
PUBMED | CROSSREF

48. Gosselin MC, Neufeld E, Moser H, Huber E, Farcito S, Gerber L, et al. Development of a new generation of high-resolution anatomical models for medical device evaluation: the Virtual Population 3.0. *Phys Med Biol* 2014;59(18):5287-303.
PUBMED | CROSSREF

49. Han M, Lee AK, Choi HD, Jung YW, Park JS. Averaged head phantoms from magnetic resonance images of Korean children and young adults. *Phys Med Biol* 2018;63(3):035003.
PUBMED | CROSSREF

50. Kim EY, Kim TJ, Goo JM, Kim HY, Lee JW, Lee S, et al. Size-specific dose estimation in the Korean lung cancer screening project: does a 32-cm diameter phantom represent a standard-sized patient in Korean population? *Korean J Radiol* 2018;19(6):1179-86.
PUBMED | CROSSREF

51. Park YS, Lee YJ, Kim W, Ji YH, Kim KB, Kang JH, et al. Image-based absorbed dosimetry of radioisotope. *Prog Med Phys* 2016;27(2):86-91.
CROSSREF